†Work presented to the Second International Positron Annihilation Conference, Kingston, Ontario (1971).
*Present address: Department of Physics, Jadavpur University, Jadavpur, Calcutta-32, India.
[1]H. S. W. Massey and C. B. O. Mohr, Proc. Phys. Soc. (London) A67, 695 (1954).
[2]I. M. Cheshire, Proc. Phys. Soc. (London) 83, 227 (1964).
[3]B. H. Bransden and Z. Jundi, Proc. Phys. Soc. (London) 92, 880 (1967).
[4]H. S. W. Massey and A. H. Moussa, Proc. Phys. Soc. (London) A77, 811 (1961).
[5]D. P. Sural and S. C. Mukherjee, Physica 49, 249 (1970).
[6]G. Ferrante and R. Geracitano, Phys. Rev. 182, 215 (1969).
[7]G. Ferrante, University of Messina, Institute of Physics Technical Report No. 5, 1967 (unpublished).
[8]J. A. Wheeler, Ann. N. Y. Acad. Sci. 48, 219 (1946).
[9]E. A. Hylleraas, Phys. Rev. 71, 491 (1947).
[10]W. Kolos, C. C. J. Roothan, and R. A. Sack, Rev. Mod. Phys. 32, 178 (1960).
[11]U. Schroeder, Z. Physik 173, 221 (1963).
[12]G. Ferrante and R. Geracitano, Nuovo Cimento Letters 3, 48 (1970).
[13]G. Ferrante, Phys. Rev. 170, 76 (1968).
[14]S. Weinbaum, J. Chem. Phys. 1, 593 (1933).
[15]A. Stancanelli and G. Ferrante, Nuovo Cimento 68B, 137 (1970).

PHYSICAL REVIEW A VOLUME 6, NUMBER 1 JULY 1972

Scattering of Intense Light by a Two-Level System

R. Gush* and H. P. Gush†
Istituto di Fisica, "Guglielmo Marconi" Università degli Studi, Rome, Italy
(Received 24 January 1972)

A general expression is found for the Green's function of a two-level system interacting with a classical monochromatic field of arbitrary frequency and intensity. The Green's function is first used to calculate the transition probability from the lower to the upper state as a function of the frequency and intensity of the field and a comparison of the results is made with experiment. It is then used to study the problem of scattering. It is found that the spectrum of the scattered radiation consists of a line at the frequency of the field (Rayleigh line) and two satellites symmetrically displaced from the Rayleigh line by an amount depending both on the intensity and frequency of the field. In addition there are emissions at three, five, etc., times the frequency of the field, and accompanying satellites. The cross sections for the production of the Rayleigh line and its satellites, and for the third-harmonic line and its satellites have been calculated for a range of values of the frequency and intensity of the incident field.

I. INTRODUCTION

A theory for the scattering of radiation by an atomic system, valid for arbitrary intensity and frequency of the incident field, has not been worked out to our knowledge. At low intensity and for off-resonance cases a low-order perturbation calculation of the cross section is adequate because the initial wave function is not substantially changed by the application of the field.[1] However, at high intensity, and particularly near resonance, the wave function may change greatly in a time comparable to the emission time for a photon because of rapid transitions induced by the field; as a result the cross section for scattering and even the spectrum of the scattered radiation is considerably different from the low-order perturbation theory prediction. The present-day availability of intense radiation fields produced by pulsed lasers makes it imperative to reexamine the problem of scattering if comparison with possible experiments is to be made.

Because an exact treatment of the problem appears impractical, one is reduced to making some simplifying assumptions. The primary one adopted here is that only two states of the atom are effective in its interaction with the radiation: That is, the atom is replaced by a two-level system endowed with an electric dipole moment. Furthermore, the energy levels are considered sharp, all relaxation processes being ignored. Apart from these two assumptions the problem of scattering is solved essentially exactly.

We start by calculating the nonrelativistic Green's-function operator for a two-level system interacting with a classical monochromatic field. This is accomplished by summing the perturbation series completely. The result, valid for arbitrary frequency and intensity of the incident field, is expressed in terms of continued fractions similar to those found by Autler and Townes[2] in their study of the dynamic Stark effect. The system is then coupled to a quantized radiation field and the probability for the spontaneous emission of a photon is

evaluated. From this probability the scattering cross section is obtained, correct to all orders in the classical field strength. In addition the allowed values of the frequency of the scattered photons are determined.

It is found that the spectrum of the scattered radiation consists of the Rayleigh line plus satellites symmetrically displaced from the Rayleigh line by an amount depending on both the intensity and the frequency ω_μ of the classical field. In addition lines are found at $3\omega_\mu$, $5\omega_\mu$, etc.; each of these lines is also accompanied by satellites. The reason for this structure is apparent when one examines the form of the square of the Green's function. For example, at resonance and at low intensities, the incident field causes the system to oscillate periodically between the lower and the upper state with a frequency $2\omega_c$, where ω_c is proportional to the matrix element of the interaction potential. Since the emission of a photon takes place primarily when the system is in the upper state, one sees that the amplitude for emission oscillates periodically with time and this causes sidebands to appear on the Rayleigh line. When the field is intense, however, the oscillation between the lower and the upper state is no longer periodic at a single frequency but components at frequencies $2\omega_\mu \pm 2\omega_c$, $4\omega_\mu \pm 2\omega_c$, etc., are also present. This permits scattering at odd multiples of ω_μ and at corresponding satellite frequencies.

The problem of scattering by a two-level system has already been treated in part by other authors.[3-6] Meyer,[6] for example, has evaluated the cross section for the Rayleigh line and the odd harmonic lines over a wide range of conditions, but has not considered the satellites. On the other hand, Stroud[3] investigates the spectrum of the scattered radiation near the Rayleigh line for the resonance case only, and does not work out the cross section. A comparison of our results with previous work will be made wherever possible.

In addition to solving the scattering problem, knowledge of the Green's-function operator makes it possible to calculate the transition probability between the two states under conditions of strong excitation. The calculations are compared with the results of an experiment of Margerie and Brossel[7] who measured, as a function of energy-level spacing, the average population of one state of a two-level system immersed in a radio-frequency field. There is over-all agreement between the theoretical and experimental results. They both exhibit, for example, three-photon absorption and the Bloch-Siegert[8] effect.

II. GREEN'S-FUNCTION OPERATOR

A. Theoretical Background

All the properties of a two-level system interacting with a classical monochromatic field may be deduced from its Green's-function operator.[9] This operator satisfies the equation

$$\left(H_0 + V(t) - i\hbar \frac{\partial}{\partial t}\right) G^+(t-t_0) = -\hbar\delta(t-t_0) \quad , \quad (2.1)$$

where H_0 is the unperturbed Hamiltonian and $V(t)$ is the interaction potential. Of the various possible ways to solve (2.1), we choose the perturbation-expansion approach using the formula

$$G^+(t-t_0) = G_0^+(t-t_0) + \hbar^{-1}\int dt'\, G_0^+(t-t')V(t')\,G_0^+(t'-t_0) + \hbar^{-2}\int\int dt'\,dt''\, G_0^+(t-t')V(t')\,G_0^+(t'-t'')V(t'')\,G_0^+(t''-t_0) + \cdots \quad , \quad (2.2)$$

where $G_0^+(t-t_0)$ is the zeroth-order Green's-function operator

$$G_0^+(t-t_0) = -\lim_{\epsilon\to 0^+} \frac{1}{2\pi}\int_{-\infty}^{\infty} d\omega_1 \frac{e^{i\omega_1(t-t_0)}}{\omega_1 - i\epsilon} \times \left(|a\rangle\langle a|\, e^{-i\omega_a(t-t_0)} + |b\rangle\langle b|\, e^{-i\omega_b(t-t_0)}\right) \quad . \quad (2.3)$$

In (2.3), the lower and upper eigenstates of the unperturbed system, $|a\rangle$ and $|b\rangle$, of eigenenergies $\hbar\omega_a$ and $\hbar\omega_b$, have been introduced. In what follows it is understood that the Green's-function operator has the form

$$G^+(t-t_0) = G_{aa}(t-t_0) + G_{bb}(t-t_0) + G_{ab}(t-t_0) + G_{ba}(t-t_0) \quad , \quad (2.4)$$

where the operators $G_{ij}(t-t_0)$ are proportional to $|i\rangle\langle j|$, with i and j each equal to either a or b. We call G_{aa} and G_{bb}, G_{ab} and G_{ba}, "diagonal" and "off-diagonal" contributions, respectively, to the Green's-function operator.

It is assumed that the interaction of the system with the external field $\vec{E}(\vec{r}, t)$ takes place through the electric dipole moment $\vec{d}$. We hence write for the interaction potential

$$V(t) = -\vec{d}\cdot\vec{E}(t) = -\vec{d}\cdot\vec{e}\,E(e^{i(\omega_\mu t+\phi)} + e^{-i(\omega_\mu t+\phi)}) \quad , \quad (2.5)$$

where ϕ is an arbitrary phase angle and $\vec{e}$ is the polarization vector. The further assumption that the matrix element of the dipole moment $\vec{d}_{ab}$ is real, permits the nonvanishing matrix elements of the interaction potential to be written

$$\langle a|V(t)|b\rangle = \langle b|V(t)|a\rangle = -\omega_c\hbar(e^{i(\omega_\mu t+\phi)} + e^{-i(\omega_\mu t+\phi)}) \quad , \quad (2.6)$$

where the frequency ω_c, given by the formula

$$\omega_c = \vec{d}_{ab} \cdot \vec{e}\, E/\hbar \ , \tag{2.7}$$

characterizes the strength of the interaction. It will frequently be convenient in the sequel to normalize other frequencies in the problem to ω_c.

A general term in the perturbation expansion for G^+ will be proportional to a contour integral of a product of factors of the type $(\omega_1 + n\omega_\mu - i\epsilon)^{-1}$, $(\omega_1 + \omega_b - \omega_a + m\omega_\mu - i\epsilon)^{-1}$, and $\omega_c e^{\pm i(\omega_\mu t_0 + \phi)}$. Referring to a description of the perturbation series using diagrams, the former two factors would be identified with propagators and the latter factors with vertex contributions. The integers n and m indicate the number of photons absorbed above the corresponding propagator. For example, the second-order contribution to G_{aa} is the following sum of four terms:

$$G''_{aa}(t-t_0) = -|a\rangle\langle a| e^{-i\omega_a(t-t_0)} \frac{1}{2\pi} \int d\omega_1 \frac{e^{i\omega_1(t-t_0)}}{\omega_1 - i\epsilon}$$
$$\times \left(\frac{\omega_c^2 e^{i2(\omega_\mu t_0 + \phi)}}{(\omega_1 + \omega_{ba} - \omega_\mu - i\epsilon)(\omega_1 - 2\omega_\mu - i\epsilon)} + \frac{\omega_c^2}{(\omega_1 + \omega_{ba} - \omega_\mu - i\epsilon)(\omega_1 - i\epsilon)} \right.$$
$$\left. + \frac{\omega_c^2}{(\omega_1 + \omega_{ba} + \omega_\mu - i\epsilon)(\omega_1 - i\epsilon)} + \frac{\omega_c^2 e^{-i2(\omega_\mu t_0 + \phi)}}{(\omega_1 + \omega_{ba} + \omega_\mu - i\epsilon)(\omega_1 + 2\omega_\mu - i\epsilon)} \right) , \tag{2.8}$$

where $\omega_{ba} = \omega_b - \omega_a$. These four terms are represented by diagrams in Fig. 1.

Each term in the perturbation expansion contains a factor of the type $e^{iN(\omega_\mu t_0 + \phi)}$ corresponding to a diagram in which there is a net emission of N photons. The contribution to G^+ corresponding to a definite value of N will be indicated by the symbol $G^{(N)}$.

To discuss the general term in the perturbation expansion we introduce the following notation for propagators: The symbol $[n, n\pm 1]$, n odd, stands for

$$(\omega_1 + \omega_{ba} + n\omega_\mu - i\epsilon)[\omega_1 + (n\pm 1)\omega_\mu - i\epsilon] \ ,$$

and the symbol $[m]$ stands for $(\omega_1 + \omega_{ba} + m\omega_\mu - i\epsilon)$ if m is odd, and $(\omega_1 + m\omega_\mu - i\epsilon)$ if m is even. The general product of propagators, to be found in $G_{aa}^{(0)}$ may be written

$$T = \frac{1}{[0]} \left(\frac{1}{[1,0]}\right)^{m_1} \left(\frac{1}{[1,2]}\right)^{m_2} \left(\frac{1}{[3,2]}\right)^{m_3} \left(\frac{1}{[3,4]}\right)^{m_4} \cdots$$
$$\times \left(\frac{1}{[-1,0]}\right)^{n_1} \left(\frac{1}{[-1,-2]}\right)^{n_2} \left(\frac{1}{[-3,-2]}\right)^{n_3} \left(\frac{1}{[-3,-4]}\right)^{n_4} \cdots , \tag{2.9}$$

where the order of perturbation equals

$$2(m_1 + m_2 + m_3 + \cdots + n_1 + n_2 + n_3 + \cdots) \ .$$

The propagators in (2.9) have been paired in the way shown to stress the fact that when $(\omega_1 + \omega_{ba} + n\omega_\mu - i\epsilon)^{-1}$ occurs then $[\omega_1 + (n\pm 1)\omega_\mu - i\epsilon]^{-1}$ also occurs. They have furthermore been ordered in the way shown because propagator pairs in a diagram such as $[1,0]^{-1}$, $[1,2]^{-1}$ or $[1,2]^{-1}$, $[3,2]^{-1}$ can be exchanged giving rise to a distinct diagram with the same over-all propagator. This decomposition of a general diagram into commuting propagator pairs permits the application of combinatorial analysis to determine the number of times $\mathfrak{N}$ a given set of propagators appears in the perturbation series[10]

$$\mathfrak{N} = \binom{m_1 + m_2 - 1}{m_2} \binom{m_2 + m_3 - 1}{m_3} \binom{m_3 + m_4 - 1}{m_4} \cdots$$
$$\times \binom{m_1 + n_1}{n_1} \binom{n_1 + n_2 - 1}{n_2} \binom{n_2 + n_3 - 1}{n_3} \cdots \ . \tag{2.10}$$

We obtain the total propagator F for $G_{aa}^{(0)}$ by summing the product $\mathfrak{N}T$ over all values of the integers m_1, m_2, etc. By repetitive use of the expression

$$\sum_n \binom{m+n-1}{n} x^n = \left(\frac{1}{1-x}\right)^m , \quad |x| < 1 \tag{2.11}$$

this sum can be performed, resulting in the continued fraction

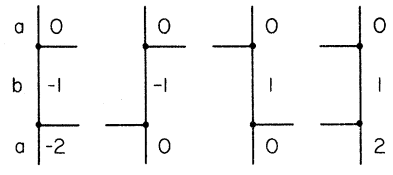

FIG. 1. Second-order diagrams contributing to G_{aa}. The letters a and b refer to the state of the two-level system, and the numbers refer to the integers n and m in the propagators $(\omega_1 + n\omega_\mu - i\epsilon)^{-1}$ and $(\omega_1 + \omega_{ba} + m\omega_\mu - i\epsilon)^{-1}$, where n is even and m is odd.

$$F = \cfrac{1}{[0] - \cfrac{1}{[1] - \cfrac{1}{[2] - \cfrac{1}{[3] - \cdots}}} - \cfrac{1}{[-1] - \cfrac{1}{[-2] - \cfrac{1}{[-3] - \cdots}}}} \quad . \tag{2.12}$$

Before expressing the Green's-function operator $G_{aa}^{(0)}$ in terms of (2.12) one must account for the fact that associated with every vertex is the product $\omega_c e^{i(\omega_\mu t_0 + \phi)}$ (or its complex conjugate). The factor ω_c is taken care of introducing the new variables $\eta = \omega_1/\omega_c$ and $\eta' = (\omega_1 + \omega_{ba})/\omega_c$, and the parameter $\mu = \omega_\mu/\omega_c$, into the perturbation expansion. The exponential part results simply in an over-all factor in $G^{(N)}$ equal to $e^{iN(\omega_\mu t_0 + \phi)}$. In the case considered at the moment N equals zero. We hence obtain

$$G_{aa}^{(0)} = -|a\rangle\langle a| e^{-i\omega_a(t-t_0)} \frac{1}{2\pi} \int d\eta\, e^{i\omega_c \eta (t-t_0)} F_a^{(0)}(\eta) \quad , \tag{2.13}$$

where

$$F_a^{(0)}(\eta) = \left[\eta - i\epsilon - \left(\frac{1}{\eta' + \mu - i\epsilon -} \; \frac{1}{\eta + 2\mu - i\epsilon -} \; \frac{1}{\eta' + 3\mu - i\epsilon -} \cdots \right) - \left(\frac{1}{\eta' - \mu - i\epsilon -} \; \frac{1}{\eta - 2\mu - i\epsilon -} \; \frac{1}{\eta' - 3\mu - i\epsilon -} \cdots \right) \right]^{-1} \quad . \tag{2.14}$$

Off-diagonal contributions to G^+ are deduced in a similar way. For example, the total propagator of $G_{ab}^{(1)}$ has the form

$$\begin{aligned} F = \sum_{m_1=1}^{\infty} \sum_{\substack{m_2, m_3, \ldots = 0 \\ n_1, n_2, \ldots = 0}}^{\infty} & \left(\frac{1}{[-1, 0]} \right)^{m_1} \binom{m_1 + m_2 - 1}{m_2} \left(\frac{1}{[-1, -2]} \right)^{m_2} \binom{m_2 + m_3 - 1}{m_3} \left(\frac{1}{[-3, -2]} \right)^{m_3} \cdots \\ & \times \binom{m_1 + n_1 - 1}{n_1} \left(\frac{1}{[1, 0]} \right)^{n_1} \binom{n_1 + n_2 - 1}{n_2} \left(\frac{1}{[1, 2]} \right)^{n_2} \cdots \\ = \left(\frac{1}{[-1] -} \; \frac{1}{[-2] -} \; \frac{1}{[-3] -} \cdots \right) & \times \left[[0] - \left(\frac{1}{[1] -} \; \frac{1}{[2] -} \; \frac{1}{[3] -} \cdots \right) - \left(\frac{1}{[-1] -} \; \frac{1}{[-2] -} \; \frac{1}{[-3] -} \cdots \right) \right]^{-1} \quad . \end{aligned} \tag{2.15}$$

$G_{ab}^{(1)}$ may hence be written as follows:

$$G_{ab}^{(1)} = -|a\rangle\langle b| e^{-i\omega_a(t-t_0)} e^{i(\omega_\mu t_0 + \phi)} \frac{1}{2\pi} \int d\eta\, e^{i\omega_c \eta (t-t_0)} F_a^{(1)}(\eta) \quad , \tag{2.16}$$

with

$$F_a^{(1)}(\eta) = \left(\frac{1}{\eta' - \mu - i\epsilon -} \; \frac{1}{\eta - 2\mu - i\epsilon -} \; \frac{1}{\eta' - 3\mu - i\epsilon -} \cdots \right) F_a^{(0)}(\eta) \quad . \tag{2.17}$$

B. Complete Green's-Function Operator

The preceding analysis can be readily extended to include contributions to the Green's function for any value of N. The complete Green's-function operators equal

$$\begin{aligned} G_{aa}(t - t_0) &= -|a\rangle\langle a| e^{-i\omega_a(t-t_0)} \frac{1}{2\pi} \int d\eta\, e^{i\omega_c \eta (t-t_0)} \sum_{n=-\infty}^{\infty} \Gamma^{2n} F_a^{(2n)}(\eta) \quad , \\ G_{ab}(t - t_0) &= -|a\rangle\langle b| e^{-i\omega_a(t-t_0)} \frac{1}{2\pi} \int d\eta\, e^{i\omega_c \eta (t-t_0)} \sum_{n=-\infty}^{\infty} \Gamma^{2n+1} F_a^{(2n+1)}(\eta) \quad , \end{aligned} \tag{2.18}$$

where $\Gamma = e^{i(\omega_\mu t_0 + \phi)}$, and where the continued fractions satisfy the following recurrence relations:

$$F_a^{(2n)}(\eta)=\left(\frac{1}{\eta\mp 2n\mu-i\epsilon-}\,\frac{1}{\eta'\mp(2n+1)\mu-i\epsilon-}\,\frac{1}{\eta\mp(2n+2)\mu-i\epsilon-}\cdots\right)F_a^{(2n\mp1)}(\eta),$$

upper sign $n>0$, lower sign $n<0$

$$F_a^{(2n\pm1)}(\eta)=\left(\frac{1}{\eta'\mp(2n+1)\mu-i\epsilon-}\,\frac{1}{\eta\mp(2n+2)\mu-i\epsilon-}\,\frac{1}{\eta'\mp(2n+3)\mu-i\epsilon-}\cdots\right)F_a^{(2n)}(\eta),\tag{2.19}$$

upper sign $n\geq 0$, lower sign $n\leq 0$.

The sum over n in (2.18) corresponds to summing over processes involving the net emission or absorption of $2n$ or $(2n+1)$ photons. The operators G_{bb} and G_{ba} are obtained from G_{aa} and G_{ab} simply by exchanging a and b everywhere (including the variable η'). In two cases the Green's-function operators (2.18) take on a simple analytic form as we now show.

1. Limiting Case $\omega_{ba}=0$

In the limiting case that ω_{ba} tends to zero the continued fractions appearing in the Green's-function operators (2.16) may be expressed in terms of known functions. In fact, using well-known properties of Bessel functions,[11] one finds that the continued fraction $F_a^{(N)}$ with $\omega_{ba}=0$, equals

$$F_a^{(N)}(\eta)=(-)^N\frac{\pi}{\mu}\,\frac{J_{-(\eta-i\epsilon)/\mu+N}(2/\mu)\,J_{(\eta-i\epsilon)/\mu}(2/\mu)}{\sin[\pi(\eta-i\epsilon)/\mu]}\ .\tag{2.20}$$

This result permits the operators themselves to be expressed in analytic form. Introducing the above formula into (2.18) and performing the contour integrals over η we obtain the following expressions:

$$\begin{aligned}G_{aa}&=-i\,|a\rangle\langle a|\,e^{-i\omega_a(t-t_0)}\textstyle\sum_n\Gamma^{2n}J_{2n}(-(4/\mu)\sin[\frac{1}{2}\omega_\mu(t-t_0)])\exp\{in[\pi+\omega_\mu(t-t_0)]\}\ \Theta(t-t_0)\ ,\\ G_{ab}&=i\,|a\rangle\langle b|\,e^{-i\omega_a(t-t_0)}\textstyle\sum_n\Gamma^{2n+1}J_{2n+1}(-(4/\mu)\sin[\frac{1}{2}\omega_\mu(t-t_0)])\exp\{i(n+\frac{1}{2})[\pi+\omega_\mu(t-t_0)]\}\ \Theta(t-t_0)\ ,\end{aligned}\tag{2.21}$$

where $\Theta(t-t_0)$ is the Heaviside step function. The operators G_{bb} and G_{ba} are obtained from (2.21) exchanging a with b. The Green's-function operator G^+ derived from (2.21) satisfies the defining equation (2.1); this verifies that the procedure of expressing the sum of the perturbation series by continued fractions is valid. The case $\omega_{ba}=0$ is of limited application in scattering problems, but it arises in the study of dynamical Stark splitting of a doubly degenerate level.[2]

2. Low-Intensity Near-Resonance Case

At sufficiently low intensity the frequency ω_c may be considered small compared to both ω_μ and ω_{ba}, and the quantities μ and $\delta=\omega_{ba}/\omega_c$ are much greater than unity. Furthermore, near resonance the quantity $|\delta-\mu|$ may be assumed much smaller than $\delta+\mu$. Under these circumstances the continued fractions can be terminated at an early stage without much error. Also, only those contributions to G^+ with N equal to 0, +1, and −1, need be considered. The Green's-function operators can hence be approximated by the following expressions:

$$G_{aa}\approx-\,|a\rangle\langle a|\,e^{-i\omega_a(t-t_0)}\,\frac{1}{2\pi}\int d\eta\,e^{i\omega_c\eta(t-t_0)}\,\frac{1}{\eta-i\epsilon-1/(\eta+\delta-\mu-i\epsilon)}\ ,\tag{2.22a}$$

$$G_{ab}\approx-\,|a\rangle\langle b|\,e^{-i\omega_a(t-t_0)}\frac{1}{2\pi}\int d\eta\,e^{i\omega_c\eta(t-t_0)}\,\frac{\Gamma}{\eta+\delta-\mu-i\epsilon}\left(\frac{1}{\eta-i\epsilon-1/(\eta+\delta-\mu-i\epsilon)}\right)\ .\tag{2.22b}$$

Expressions for G_{bb} and G_{ba} are obtained from (2.22) by exchanging a with b, changing the sign of δ and μ, and replacing Γ with its complex conjugate.

We will require the poles and residues of the propagators in the above Green's functions. Introducing the quantity $\gamma=\delta-\mu$, the poles of G_{aa} are located at

$$P^a_{0,\pm1}=\tfrac{1}{2}[-\gamma\pm(\gamma^2+4)^{1/2}]+i\epsilon\ ,\tag{2.23}$$

and the corresponding residues are

$$R(aa\,|\,0,\pm1,0)=\tfrac{1}{2}[1\pm\gamma(\gamma^2+4)^{-1/2}]\ .\tag{2.24}$$

The notation introduced here for the pole location and the residue will be explained in detail later. The propagator in G_{ab} has poles at the same place as the propagator in G_{aa}; however, the residues are different:

$$R(ab\,|\,0,\pm1,1)=\pm(\gamma^2+4)^{-1/2}\ .\tag{2.25}$$

In the case of G_{bb} and G_{ba} the quantities corresponding to those listed above are

$$P^{b}_{0,\pm 1} = \tfrac{1}{2}[\gamma \pm (\gamma^2+4)^{1/2}] + i\epsilon \ , \qquad (2.26a)$$

$$R(bb\,|\,0,\pm 1,0) = \tfrac{1}{2}[1 \mp \gamma(\gamma^2+4)^{-1/2}] \ , \qquad (2.26b)$$

$$R(ba\,|\,0,\pm 1,-1) = \pm(\gamma^2+4)^{-1/2} \ . \qquad (2.26c)$$

Using the above results it follows that the probability to find the system in the state $|b\rangle$ having started at time t_0 in the state $|a\rangle$ equals

$$W_{ba} = 4(\gamma^2+4)^{-1}\sin^2[\tfrac{1}{2}\omega_c(\gamma^2+4)^{1/2}(t-t_0)] . \qquad (2.27)$$

This is the same result as that obtained from the rotating-wave approximation[2] which means that the approximations made at the beginning of this section are equivalent to those made in the rotating-wave analysis.

Before proceeding to discuss the poles and residues of the exact Green's function we would like to make the following remark. Because the system under consideration has an explicitly time-dependent Hamiltonian, it does not possess stationary states and energy eigenvalues in the usual sense. However, in certain circumstances the system behaves as if it possessed an energy-level spectrum. The latter may be obtained in an evident way from the poles of the Green's function. In the weak-field case, using (2.23) and (2.26a), one finds for the spectrum

$$(E_a)_{\mp} = \{\omega_a + \tfrac{1}{2}(\omega_{ba}-\omega_\mu) \mp [\tfrac{1}{4}(\omega_{ba}-\omega_\mu)^2+\omega_c^2]^{1/2}\}\hbar \ , \qquad (2.28)$$

$$(E_b)_{\mp} = \{\omega_b - \tfrac{1}{2}(\omega_{ba}-\omega_\mu) \mp [\tfrac{1}{4}(\omega_{ba}-\omega_\mu)^2+\omega_c^2]^{1/2}\}\hbar \ .$$

At resonance the energy spectrum consists of two doublets located at $(\omega_a \pm \omega_c)\hbar$ and $(\omega_b \pm \omega_c)\hbar$. These doublets may be considered to arise from the dynamic Stark effect; their location is the same as that given by Townes and Schawlow,[12] who used a different type of analysis. The above energy-level structure makes it very plausible that radiation emitted by a two-level system illuminated by a field resonant with it should consist of a component at frequency ω_μ and satellite components at frequencies $\omega_\mu \pm 2\omega_c$. This guess is confirmed by a detailed calculation to be discussed later.

3. *Poles of Exact Green's-Function Operator*

The behavior of the continued fractions in the exact Green's-function operators (2.18) was investigated numerically using a digital computer because analytic treatment did not seem feasible. Since the continued fractions appear in a contour integral their important properties are the pole locations and the residues at the poles. The approximate location of two poles (2.23) was already known analytically. These locations were taken as initial values in an iterative procedure which converged to the true pole locations. It was found that in addition to the two poles mentioned the continued fractions have poles separated from these by $2n\mu$, n being a negative or positive integer. However, the residues become rapidly smaller with increasing n and at the highest intensity considered it was adequate to take into account a total of 14 poles. For the same reason the maximum value of $|N|$ taken into account was 6. In the analysis the continued fraction was terminated at a certain level; the lowest level which it was necessary to include was determined empirically so that the addition of another level made no significant change in the pole locations and the residues. The required depth in the continued fraction was a function of the intensity, being greater the higher the intensity.

The computer program was verified in two ways: The first was to check that in the case $\omega_{ba} = 0$ the residues computed from the continued fractions agreed with those evaluated using the analytic expression (2.20). The second was to sum the residues over all poles taken into consideration for a given N: For $|N| > 0$ one obtained zero, and for $N = 0$ one obtained unity. This is a necessary condition that at time $t = t_0$ no transition has taken place.

All the poles of the continued fractions can, in fact, be found from the location of one of them. If a pole is located, say at η_p, then the others are located at exactly $\eta_p + 2n\mu$ and $-\eta_p - \gamma + 2n\mu$, where n is a positive or negative integer and where $\gamma = (\omega_{ba}-\omega_\mu)/\omega_c$. The pole locations of G_{aa} and G_{ab} are the same, and those of G_{bb} and G_{ba} are obtained from them by reversing the sign. A typical set of pole locations is shown in Fig. 2 from which we see that these may be expressed by the following formulas:

$$P^{a}_{m,\alpha} = -\tfrac{1}{2}\gamma + \alpha\zeta + 2m\mu \ ,$$
$$P^{b}_{m,\alpha} = \tfrac{1}{2}\gamma + \alpha\zeta + 2m\mu \ . \qquad (2.29)$$

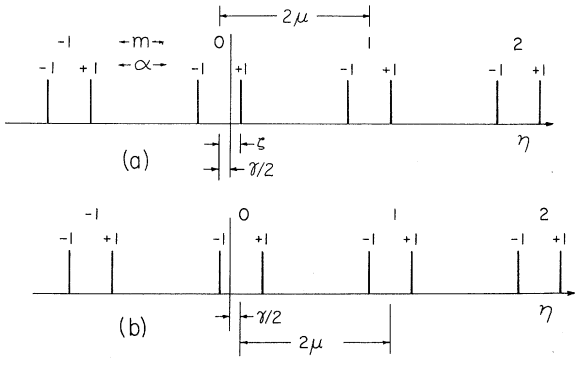

FIG. 2. (a) Pole locations along the η axis of the continued fractions occurring in G_{aa} and G_{ab}. The indices m and α label the poles. (b) The pole locations of G_{bb} and G_{ba} for the same values of μ and γ as used in (a).

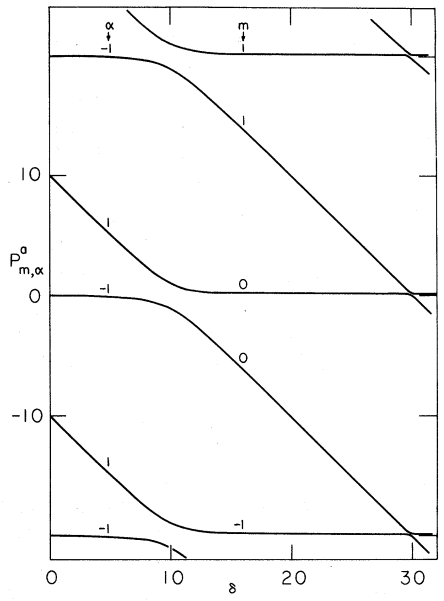

FIG. 3. Pole locations of G_{aa} as a function of δ for the case $\mu = 10$.

The superscripts a and b mean that one is referring to poles of G_{aa} or G_{bb}, respectively, whereas the subscript m is a positive or negative integer, and α can have the values ± 1 only. The quantity ζ, which must be determined numerically, depends on both μ and γ. At low intensity there are only two poles of importance; in the resonance condition they are located at $\eta = \pm 1$. We choose arbitrarily ζ equal to unity and assign to the pole at $\eta = 1$ the suffixes $m = 0$, $\alpha = 1$, and to the pole at $\eta = -1$ the suffixes $m = 0$, $\alpha = -1$. [These conventions have been used in (2.23) and (2.26a).] This labeling follows the poles even though they shift when off-resonance and high-intensity conditions prevail.

The location of the poles of G_{aa} as a function of $\delta = \omega_{ba}/\omega_c$ is shown in Fig. 3 for $\mu = 10$ and in Fig. 4 for $\mu = 2$, corresponding to two values of the intensity of the classical field. We note that the pole location curves never cross as ω_{ba} is varied for a fixed ω_μ. However, the poles approach one another very closely at regions of resonance when $\omega_{ba} \approx (2n+1)\omega_\mu$, n integral: care must be taken not to jump unwittingly from one curve to another in the numerical analysis. If Figs. 3 and 4 are compared with Fig. 1 of the article by Meyer[6] (a relativistic field-theoretical treatment of the scattering problem), it will be immediately recognized that his parameter h is equivalent to the pole location of the Green's function. Similarly, a comparison with the work of Autler and Townes[2] shows that the pole locations are equivalent to the allowed values of a parameter λ introduced in a trial solution of the Schrödinger equation.

Using the notation introduced in (2.29) for the pole locations the Green's-function operators (2.18) may be expressed as a sum over simple poles in the following way:

$$G_{ij} = -|i\rangle\langle j| e^{-i\omega_i(t-t_0)} \times \frac{1}{2\pi}\int d\eta\, e^{i\omega_c\eta(t-t_0)} \sum_{m,\alpha,\beta} \frac{R(ij|m,\alpha,\beta)\Gamma^\beta}{\eta - P^i_{m,\alpha} - i\epsilon} . \quad (2.30)$$

The symbol $R(ij|m, \alpha, \beta)$ stands for the residue of the continued fraction $F_i^{(\beta)}(\eta)$ at the pole $P^i_{m,\alpha}$. In (2.30), the indices i and j can each be either a or b. We note that if $i = j$, β must be even, and if $i \neq j$, β is odd. This form of the Green's-function operator will be used in subsequent calculations.

III. MARGERIE-BROSSEL EXPERIMENT

The Green's-function operator can be used to calculate the probability that a two-level system, suddenly immersed in an oscillating field, makes a transition from the lower to the upper state. This probability equals

$$W_{ba} = |\langle b|G^+(t-t_0)|a\rangle|^2 = \Big|\sum_{m,\alpha,\beta} \Gamma^\beta R(ba|m,\alpha,\beta)\exp\{i\omega_c P^b_{m,\alpha}(t-t_0)\}\Big|^2 . \quad (3.1)$$

At low intensity, only for two poles do the residues appearing in (3.1) have appreciable values and one obtains the sinusoidal variation of W_{ba} with time already expressed in Eq. (2.27). At high intensity many other poles contribute, with the result that higher-frequency components are added to the main sinusoidal pattern. Such patterns have already been calculated by Salzman,[13] who numerically integrated the Schrödinger equation for a two-level

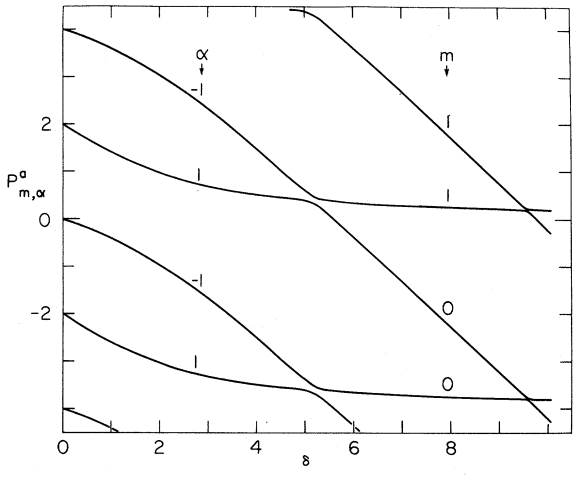

FIG. 4. Pole locations of G_{aa} as a function of δ for the case $\mu = 2$.

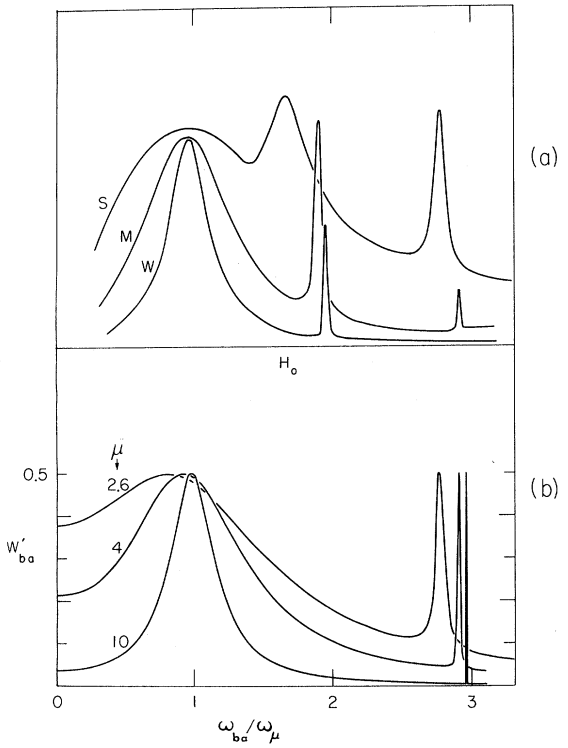

FIG. 5. Results of the experiment of Margerie and Brossel (Ref. 7) reproduced from their Fig. 2. The symbols S, M, and W stand for strong medium and weak field strength $\vec{H}_1$, respectively. The level spacing is proportional to $\vec{H}_0$. (b) The calculated probability W'_{ba} as a function of the level spacing for three different values of the quantity μ.

system with a sinusoidal perturbation.

The average probability that a system is in the upper state $|b\rangle$ having started at an uncertain time in state $|a\rangle$ is equal to the time-independent part of (3.1):

$$W'_{ba} = \sum_{m,\alpha,\beta} R(ba\,|\,m,\alpha,\beta)^2 . \qquad (3.2)$$

An interesting comparison of this formula can be made with an experiment of Margerie and Brossel.[7] Atoms of sodium in a uniform static magnetic field $\vec{H}_0$ were prepared in a definite m state of an excited level by absorption of polarized optical radiation. A radio-frequency field $\vec{H}_1$ of fixed frequency promoted transitions to an adjacent state of quantum number $(m+1)$. The intensity of the emitted light of a particular polarization, proportional to the population of this state, was measured as a function of the strength of the static magnetic field, that is, as a function of the level spacing. Because this experiment may be rather closely described in terms of a two-level system, the signal intensity may be compared to W'_{ba}. However, one detail cannot be included in our model: a component of the oscillating field along the direction of $\vec{H}_0$. This additional field has the effect of modulating the level spacing and permitting transitions not allowed in our case.

In Fig. 5(a), are shown the experimental results taken at three different radio-frequency powers. In Fig. 5(b), are shown the calculated spectra, the intensities being chosen empirically to obtain the best agreement with the three curves of Fig. 5(a). The experimental curves show a broad main resonance plus two narrower resonances, one of which occurs as a result of two-photon absorption, the other being due to three-photon absorption. The calculated curve shows the main resonance plus the three photon absorption peak only. The two-photon absorption process occurs experimentally because, as mentioned previously there is a component of the exciting field parallel to $\vec{H}_0$.[14] Neglecting this discrepancy there is good over-all agreement between the observed and calculated spectra. The location and width of the three-photon absorption peak are the same in the observed and calculated spectra corresponding to the two higher intensities. However, in the lowest intensity case the peak was missed experimentally presumably due to the very small width. The three-photon absorption peak is shifted in frequency from the location $\omega_{ba} = 3\omega_\mu$ by the Bloch-Siegert effect. From the amount of the shift it would be possible in principle to deduce the transition dipole moment, were it not known already from other considerations.

IV. CROSS SECTION FOR SCATTERING

The two-level system is now coupled to a quantized field via the electric dipole moment. Since we are interested in photon emission the effective part of the interaction Hamiltonian may be written

$$H_I = i(2V)^{-1/2} \sum_\lambda \vec{d}\cdot\vec{e}_\lambda\, \omega_\lambda^{1/2} b_\lambda^\dagger e^{i\omega_\lambda t} , \qquad (4.1)$$

where λ specifies a field mode of frequency ω_λ and momentum $\vec{\kappa}_\lambda$ and $\vec{e}_\lambda$ is the polarization vector. $b_\lambda^\dagger$ is the creation operator for the field and V the quantization volume. We choose units so that $c = \hbar = 1$.

This interaction potential introduces a change in the Green's-function operator equal to

$$\Delta G = \int dt'\, G^+(t-t')\, H_I(t')\, G^+(t'-t_0) , \qquad (4.2)$$

where we have chosen as zero-order Green's functions the exact Green's function for the two-level system in the classical field. The amplitude for emission of a photon may be deduced from ΔG.

The probability that the system starting at time t_0 in state $|l\rangle$ is at time t in state $|i\rangle$ having emitted a photon of type $\vec{\kappa}$ equals

$$|S_{il}|^2=\left|\left(\frac{2\omega_\kappa}{V}\right)^{1/2}\sum_{j\neq k}\vec{d}_{jk}\cdot\vec{e}_\kappa\sum_{m,\ldots,\beta'}R(ij|m\alpha\beta)R(kl|m'\alpha'\beta')\,\Gamma^{\beta+\beta'}\right.$$
$$\times\exp\{i\tfrac{1}{2}\omega_c[P^i_{m\alpha}+P^k_{m'\alpha'}-(1/\omega_c)(\omega_{ki}-\omega_\kappa-\beta\omega_\mu)](t-t_0)\}$$
$$\left.\times\frac{\sin\{\frac{1}{2}\omega_c[P^i_{m\alpha}-P^k_{m'\alpha'}+(1/\omega_c)(\omega_{ki}-\omega_\kappa-\beta\omega_\mu)](t-t_0)\}}{\omega_c[P^i_{m\alpha}-P^k_{m'\alpha'}+(1/\omega_c)(\omega_{ki}-\omega_\kappa-\beta\omega_\mu)]}\right|^2, \quad (4.3)$$

which we have obtained from (4.2) using the explicit form for G^+ given in (2.30).

We will be interested in deducing from $|S_{il}|^2$ a cross section for scattering which is independent of the time. This means that only those terms of $|S_{il}|^2$ obeying the following restrictions are of interest:

$$P^i_{m\alpha}-P^k_{m'\alpha'}+(1/\omega_c)(\omega_{ki}-\beta\omega_\mu)$$
$$=P^i_{m''\alpha''}-P^{k'}_{m'''\alpha'''}+(1/\omega_c)(\omega_{k'i}-\beta''\omega_\mu)\,, \quad (4.4a)$$
$$P^i_{m\alpha}+P^k_{m'\alpha'}-(1/\omega_c)(\omega_{ki}-\beta\omega_\mu)$$
$$=P^i_{m''\alpha''}+P^{k'}_{m'''\alpha'''}-(1/\omega_c)(\omega_{k'i}-\beta''\omega_\mu)\,, \quad (4.4b)$$
$$\beta+\beta'=\beta''+\beta'''\,, \quad (4.4c)$$

where $m'',\ldots,\beta'''$, k' are additional indices introduced by the square in (4.3). The relevant part of $|S_{il}|^2$ hence equals

$$|S'_{il}|^2=2V^{-1}(\vec{d}_{ab}\cdot\vec{e}_\kappa)^2\omega_\kappa\sum_{j\neq k}\sum_{j'\neq k'}{\sum}'R(ij|m\alpha\beta)R(kl|m'\alpha'\beta')R(ij'|m''\alpha''\beta'')R(k'l|m'''\alpha'''\beta''')$$
$$\times\left(\frac{\sin\{\frac{1}{2}\omega_c[P^i_{m\alpha}-P^k_{m'\alpha'}+(1/\omega_c)(\omega_{ki}-\omega_\kappa-\beta\omega_\mu)](t-t_0)\}}{\omega_c[P^i_{m\alpha}-P^k_{m'\alpha'}+(1/\omega_c)(\omega_{ki}-\omega_\kappa-\beta\omega_\mu)]}\right)^2. \quad (4.5)$$

In (4.5), the meaning of the symbol $\sum'$ is that summations are carried out over only those values of the indices m, $\alpha,\ldots,\beta'''$, for which the restrictions (4.4) are satisfied.

For large times $t-t_0$, the last factor in (4.5) acts like a δ function in the variable ω_κ. There are hence contributions to the cross section only over small ranges of ω_κ centered on

$$\omega_\kappa=\omega_c(P^i_{m\alpha}-P^k_{m'\alpha'})+\omega_{ki}-\beta\omega_\mu\,. \quad (4.6)$$

Introducing the expressions (2.29) for the pole locations into (4.6) (and taking into account the fact that if $i=k$, β must be odd, and if $i\neq k$, β must be even), we see that the possible frequencies for spontaneous emission are

$$\omega_\kappa=\omega_\mu\,,\ 3\omega_\mu\,,\ 5\omega_\mu\,,\ldots,\ \text{etc.},$$
$$\omega_\kappa=\omega_\mu\pm2\xi\omega_c\,,\ 3\omega_\mu\pm2\xi\omega_c\,,\ 5\omega_\mu\pm2\xi\omega_c\,,\ldots,\ \text{etc.} \quad (4.7)$$

That is, the spectrum of the scattered light consists of the Rayleigh line at $\omega_\kappa=\omega_\mu$, accompanied by two satellites symmetrically displaced to higher and lower frequency, plus lines and accompanying satellites at the odd harmonics $3\omega_\mu$, $5\omega_\mu$, etc.[15]

If it is assumed that the system starts in state $|a\rangle$, and we are not interested in the final state, the cross section for scattering at one of the allowed values of ω_κ equals

$$\sigma(\omega_\kappa)=\frac{\omega_\mu V}{(2\pi)^3 I}\int d^3\kappa\left(\frac{d}{dt}(|S_{aa}|^2+|S_{ba}|^2)\right)$$
$$=A_\kappa\sum_{j\neq k}\sum_{j'\neq k'}{\sum}''[R(aj|m\alpha\beta)R(ka|m'\alpha'\beta')R(aj'|m''\alpha''\beta'')R(k'a|m'''\alpha'''\beta''')$$
$$+R(bj|m\alpha\beta)R(ka|m'\alpha'\beta')R(bj'|m''\alpha''\beta'')R(k'a|m'''\alpha'''\beta''')], \quad (4.8)$$

where

$$A_\kappa=\frac{\pi\omega_\mu\omega_\kappa^3}{(2\pi)^3 I}\int d\Omega_\kappa\,(\vec{d}_{ab}\cdot\vec{e}_\kappa)^2 \quad (4.9)$$

and $I=E^2/2\pi$ is the intensity of the classical field. The meaning of the symbol $\sum''$ is that not only is the sum over m, $\alpha,\ldots,\beta'''$, restricted by the conditions (4.4) but also by the condition (4.6) where ω_κ has the desired value. The quantity $d\Omega_\kappa$ in (4.9) is an element of solid angle into which the photon is emitted.

An analytic expression for $\sigma(\omega_\kappa)$ may be obtained in the low-intensity case introducing the residues (2.24), (2.25), (2.26b), and (2.26c) into (4.8) and applying the restrictions (4.4). We obtain for the cross sections of the Rayleigh line and its two satellites

$$\sigma(\omega_\kappa=\omega_\mu)=A_\kappa(\gamma^2+4)^{-1}\,,$$

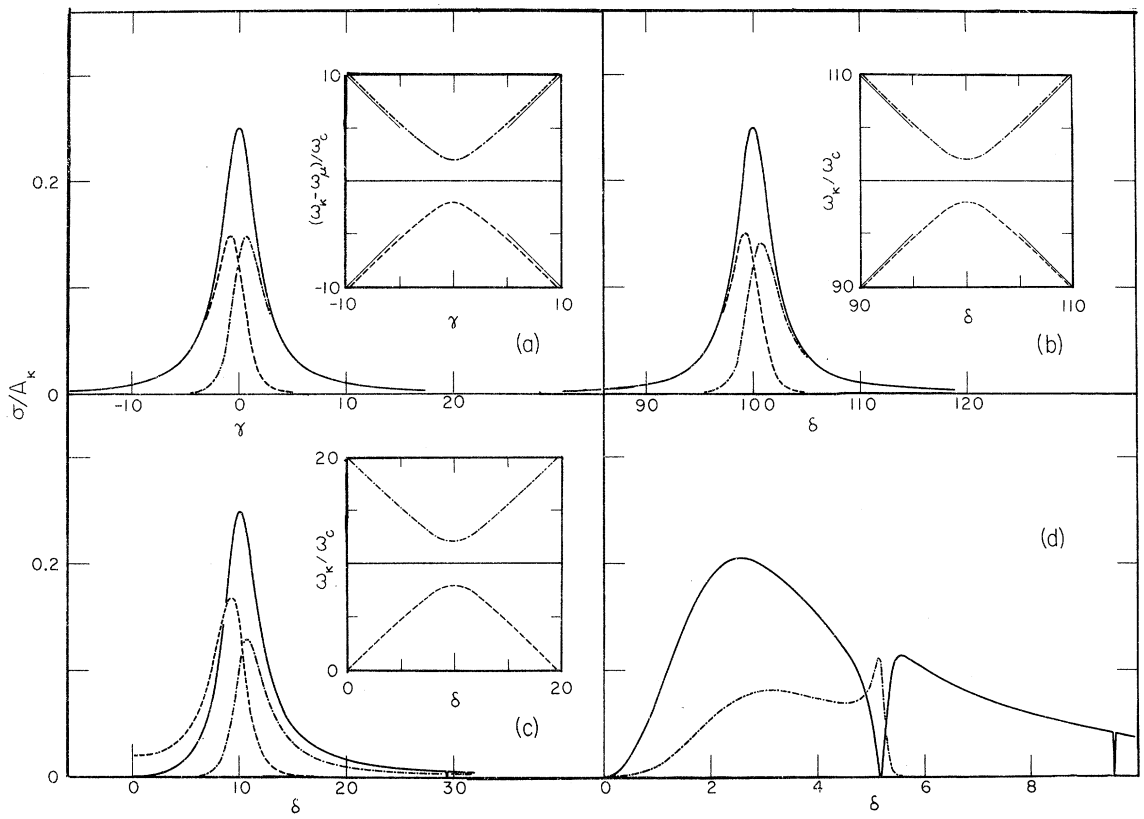

FIG. 6. (a) Quantities σ/A_κ as a function of γ calculated from (4.10). The solid curve refers to the Rayleigh cross section, the dashed curve to the cross section for the lower frequency satellite, and the dot-dashed curve to the cross section for the upper frequency satellite. The spectrum of the scattered radiation as a function of γ is shown in the inset. (b) σ/A_κ for the case $\mu=100$, shown as a function of δ. (c) σ/A_κ for the case $\mu=10$. (d) σ/A_κ for the Rayleigh line and for the higher-frequency satellite in the case $\mu=2$.

$$\sigma(\omega_\kappa=\omega_\mu+\omega_c(\gamma^2+4)^{1/2}) = \tfrac{1}{2}A_\kappa[(\gamma^2+4)^{-1}+\gamma(\gamma^2+4)^{-3/2}],$$
$$\sigma(\omega_\kappa=\omega_\mu-\omega_c(\gamma^2+4)^{1/2}) = \tfrac{1}{2}A_\kappa[(\gamma^2+4)^{-1}-\gamma(\gamma^2+4)^{-3/2}], \qquad (4.10)$$

where A_κ is deduced in each case from formula (4.9), introducing the appropriate frequency ω_κ.

The three cross sections above, divided by A_κ, are shown as functions of γ in Fig. 6(a). It can be seen from this figure that at resonance the intensity of each of the satellite lines equals one-half the intensity of the Rayleigh line (apart from the factor ω_κ^3 contained in A_κ). This is in agreement with the results of Stroud,[3] Mollow,[4] and Newstein.[5] However, off resonance, the intensity of one satellite grows relative to the other and becomes approximately equal to the intensity of the Rayleigh line. This is in disagreement with Mollow[4] who predicts that the satellites always have equal intensity. Because the value of $\sigma(\omega_\mu)/A_\kappa$ at resonance is independent of the value of ω_c, the intensity of radiation scattered by the two-level system under the resonance condition is independent of the intensity of the classical field. That is, it is not possible to force the system to emit more radiation by increasing the driving field strength. (These remarks would have to be modified, naturally, for very low intensities, where the spontaneously emitted field strength is comparable to the classical field strength.) Off resonance, the amount of scattering is intensity dependent, but saturation also takes place.

In the inset of Fig. 6(a) the frequencies of the scattered radiation ω_κ/ω_c are plotted. The frequency of the satellite which is most intense in the off-resonance case approaches asymptotically ω_{ba}. What this means is that in an off-resonance scattering experiment only two strong features will be observed, one at frequency ω_μ and the other near ω_{ba}. The latter could be mistaken for simple fluoresence were it not for the presence of a frequency shift, the magnitude of which is intensity dependent. A measurement of this shift combined with a knowledge of the incident-field strength would

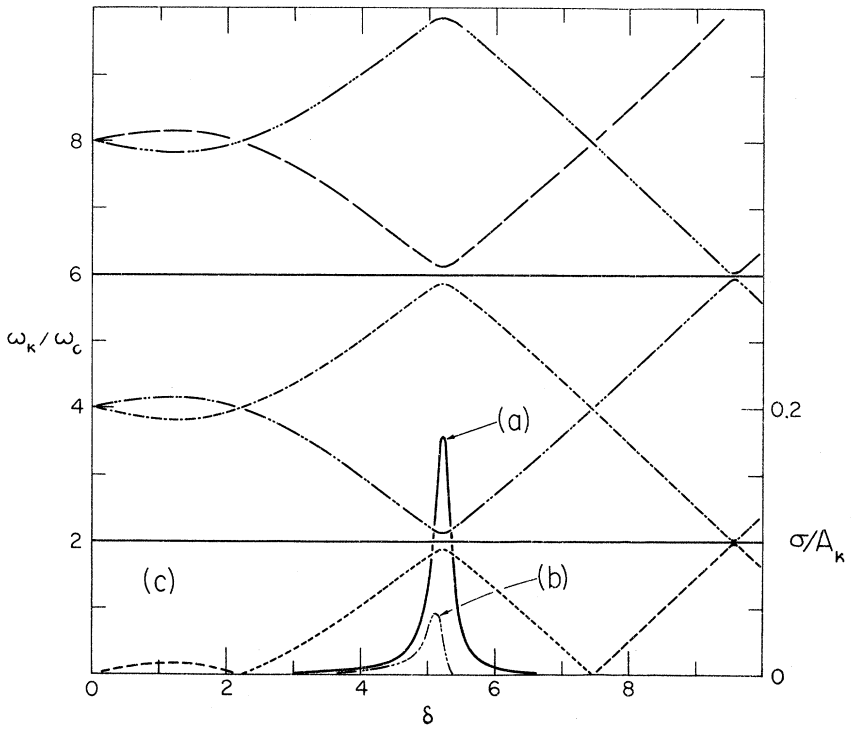

FIG. 7. (a) Quantity σ/A_κ for the third-harmonic line at $\omega_\kappa = 3\omega_\mu$, for the case $\mu = 2$. (b) σ/A_κ for the satellite at frequency $\omega_\kappa = 3\omega_\mu - 2\omega_c\xi$. (c) Frequencies of scattering for the case $\mu = 2$. The Rayleigh and the third-harmonic frequencies are shown by solid lines. Dashed and dot-dashed lines indicate the frequency of satellite lines.

yield a value for the transition dipole moment.

Cross sections were also computed using residues obtained from the numerical analysis of the continued fractions. Four values of μ were chosen: 1000, 100, 10, and 2. For the case of $\mu = 1000$ the result was indistinguishable from Fig. 6(a). For $\mu = 100$, 10, and 2, the results are shown in Figs. 6(b)–6(d), respectively.[16] Comparison of Figs. 6(a) and 6(b) show that although there are differences in the cross sections for the satellites, these differences are small and one may conclude that for $\mu \gtrsim 100$ the analytic form for the cross section may be used. However, for $\mu < 100$ the analytic results are quite inadequate to describe the scattering cross section.

The value of μ reached in a practical experiment depends of course on the system chosen. If one works in the optical region of the spectrum then μ would probably be greater than about 50. The latter corresponds to light from a ruby laser slightly focused to obtain a power of 10^{10} W/cm^2 and to a transition dipole moment of 5×10^{-18} esu cm. Higher power levels, although desirable from the point of view of producing nonlinear effects, might easily result in a breakdown of the system studied. Experiments in the domain $\mu \sim 2$ will probably require the use of high-power lasers in the infrared.

Whereas for low intensity ($\mu \gtrsim 100$) the shape of the cross section for the Rayleigh line as a function of $(\omega_{ba} - \omega_\mu)/\omega_c$ is nearly Lorentzian, this is no longer the case for $\mu \lesssim 10$. The curve is skewed and furthermore shows a dip near $\omega_{ba} = 3\omega_\mu$. This dip is very sharp for $\mu = 10$ but more obvious for $\mu = 2$. In the latter case one also sees a dip near $\omega_{ba} = 5\omega_\mu$. These dips are due to scattering taking place predominantly at frequencies near $\omega_\kappa = 3\omega_\mu$ and $5\omega_\mu$.

The cross section for scattering at $\omega_\kappa = \omega_\mu$ is identical with that of Meyer[6] for the two cases $\mu = 10$ and $\mu = 2$ ($z = 0.1$ and 0.5, respectively, in his Fig. 2). This shows the equivalence of our two substantially different approaches to this problem. As pointed out previously he makes no mention of the satellites.

The cross section for scattering at $\omega_\kappa = 3\omega_\mu$ is shown in Fig. 7(a) for the case $\mu = 2$ only. For lower intensity cases the width of the cross-section curve becomes rapidly smaller as has already been indicated by Meyer.[6] It is approximately equal to the width of the three-photon absorption feature in W'_{ba}, examples of which are shown in Fig. 5. The cross section for scattering at $\omega_\kappa = 3\omega_\mu - 2\omega_c\xi$ is shown in Fig. 7(b). The satellite at $\omega_\kappa = 3\omega_\mu + 2\omega_c\xi$ has a relatively small cross section and is not plotted. The peak in all these cross sections occurs at a frequency ω_{ba} smaller than $3\omega_\mu$. This shift in the frequency of the resonance is similar to the Bloch-Siegert effect already mentioned in connection with the experiment of Margerie and Brossel.[7]

The frequencies of the scattered radiation for

the case $\mu = 2$ are plotted as a function of δ in Fig. 7(c). It is evident that the spectrum in the high-intensity case is quite complex, consisting of many lines of which the exact frequency and intensity depends strongly on ω_{ba}. For example, it should be noticed that the satellite of the Rayleigh line at frequency $\omega_\kappa = \omega_\mu + 2\omega_c\zeta$, and the satellite of the fifth harmonic at frequency $5\omega_\mu - 2\omega_c\zeta$, lie close in frequency to the third-harmonic line at $\omega_\kappa = 3\omega_\mu$, when ω_{ba} is near $3\omega_\mu$. This means that the spectrum of the scattered radiation in the region $\omega_\kappa \approx 3\omega_\mu$ will consist of a close triplet. Since the cross sections and frequencies are strongly intensity dependent it is difficult to make a general statement about the spectrum; for each value of μ a separate calculation would be required.

In conclusion one may remark that the study of light scattered from an intense monochromatic source by a two-level system (or by an atomic system which approximates a two-level system) should show many interesting nonlinear effects such as the appearance of satellites on the Rayleigh line and harmonic generation. The measurement of these effects would yield information on the transition dipole moment of the system.

ACKNOWLEDGMENT

The authors would like to thank Professor S. Cunsolo for his kind hospitality while this work was being done.

---

*Permanent address: 4639 W-10th Vancouver, British Columbia.

†Permanent address: Department of Physics, University of British Columbia, Vancouver, British Columbia.

[1]H. A. Kramers, *Quantum Mechanics* (Dover, New York, 1946).

[2]S. H. Autler and C. H. Townes, Phys. Rev. 100, 703 (1955).

[3]C. R. Stroud, Jr., Phys. Rev. A 3, 1044 (1971).

[4]B. R. Mollow, Phys. Rev. 188, 1969 (1969).

[5]M. C. Newstein, Phys. Rev. 167, 89 (1968).

[6]J. W. Meyer, Phys. Rev. A 3, 1431 (1971).

[7]J. Margerie and J. Brossel, Compt. Rend. 241, 373 (1955).

[8]F. Bloch and A. Siegert, Phys. Rev. 57, 522 (1940).

[9]P. Roman, *Advanced Quantum Theory* (Addison-Wesley, Reading, Mass., 1965).

[10]Some discussion of this procedure will be found in Z. Fried and J. H. Eberly, Phys. Rev. 136, B871 (1964); and R. Gush and H. P. Gush, Phys. Rev. D 3, 1712 (1971).

[11]M. Abramowitz and I. Stegun, *Handbook of Mathematical Functions* (Dover, New York, 1965), pp. 363, 361, and 360.

[12]C. H. Townes and A. L. Schawlow, *Microwave Spectroscopy* (McGraw-Hill, New York, 1955).

[13]W. R. Salzman, Phys. Rev. Letters 26, 220 (1971).

[14]J. Winter, Compt. Rend. 241, 375 (1955).

[15]When one goes off resonance ζ varies considerably, as may be seen from Fig. 3, keeping in mind that $\zeta = \frac{1}{2}(p^a_{m,1} - p^a_{m,-1})$. However, ζ never exceeds μ. In off-resonance conditions it may thus happen that $2\zeta\omega_c$ is greater than ω_μ. In such a case the formula for ω_κ (4.7), second line, should read: $\omega_\kappa = \pm\omega_\mu + 2\zeta\omega_c$, $3\omega_\mu \pm 2\zeta\omega_c$, $5\omega_\mu \pm 2\zeta\omega_c$, etc.

[16]In Fig. 6(d), the quantity σ/A_κ has not been plotted for the lower-frequency satellite since the frequency is sufficiently small that σ is, in fact, negligible compared to σ ($\omega_\kappa = \omega_\mu$).